



Field-emission properties of carbon nanotube composite in side-electron emission configuration

Kishi, Naohiro
Kita, Takashi
Magario, Akira
Noguchi, Toru

(Citation)

JOURNAL OF APPLIED PHYSICS, 109(7):074307-074307

(Issue Date)

2011-04-11

(Resource Type)

journal article

(Version)

Version of Record

(URL)

<https://hdl.handle.net/20.500.14094/90001368>



Field-emission properties of carbon nanotube composite in side-electron emission configuration

Naohiro Kishi,¹ Takashi Kita,^{1,a)} Akira Magario,² and Toru Noguchi²¹*Department of Electrical and Electronic Engineering, Graduate School of Engineering, Kobe University, 1-1 Rokkodai, Nada, Kobe 657-8501, Japan*²*Akira Magario and Toru Noguchi, Nisshin Kogyo Co., Ltd., 40 Kokubu, Ueda, Nagano 836-8505, Japan*

(Received 5 October 2010; accepted 22 February 2011; published online 6 April 2011)

Field-emission characteristics of a carbon nanotube (CNT)/elastomer composite have been investigated. We performed theoretical calculations of the field distribution in a field emission device structure with the side-electron configuration of the composite sheet. According to the calculation results, the electric field is found to be concentrated at the edge of the composite sheet which leads to an enhancement of the local electric field at the CNT tips protruding from the composite. Furthermore, we calculated the trajectories of emitted electrons. From the obtained results, bright luminescence over 37000 cd/m² from green phosphor was obtained by optimizing the electrode structure. © 2011 American Institute of Physics. [doi:10.1063/1.3567913]

I. INTRODUCTION

Carbon nanotube (CNT) composites, in which CNTs are homogeneously dispersed in an appropriate supporting matrix, have been attracting considerable interest due to their enhanced thermal, mechanical, and electrical properties.^{1–5} Generally, various types of plastics such as polystyrene, polypropylene, and elastomers are used as matrix materials. Particularly in the case of elastomers, the electrical conductivity is found to considerably reduce by employing CNTs; this property is expected to introduce new applications of CNTs in flexible, large-scale devices.^{6–8} Recently, we demonstrated efficient electron emission from such conductive CNT/elastomer composites.⁶ CNTs are being considered as potential cold cathode materials for next-generation high-performance lighting devices.^{9,10} The excellent electron emission characteristics of various CNTs fabricated on solid-state substrates have already been demonstrated.^{11,12} On the other hand, CNT composites used as cathodes are thermally more stable during operation as compared to free-standing CNTs on a substrate in vacuum because of the relatively high thermal conductivity of the composites. Therefore, arbitrarily shaped, long-life, high-stability cold cathodes are expected to be realized using CNT composites. A similarly efficient electron emission has been observed in the case of composites of thick multiwalled CNTs, or the so-called carbon nanofibers, dispersed in elastomer matrixes such as natural rubber and ethylene propylene diene monomer (EPDM) rubber.⁷

Generally, electron emission can be obtained using triode- or diode-type device structures, where the cathodes and anodes are arranged facing each other and separated by an insulating spacer. The conventional device structure requires a transparent electrode such as an indium-tin-oxide (ITO) glass sheet and a narrow uniform vacuum space

between the electrodes. The fabrication of large-scale, flexible, ITO-free field-emission devices involves certain issues that need to be resolved. We have proposed a device structure with a side-electron emission configuration, in which electrons are emitted from the cross-sectional side of the composite sheet.^{7,13} To achieve efficient electron emission in this configuration, optimization of the detailed field emission processes is necessary. In this work, we calculated the field distribution in case of the field-emission device structure with the side-electron emission configuration of a CNT/elastomer composite sheet. According to our calculation results, we analyzed experimental field-emission characteristics and optimized the electrode structure of the field-emission device for realizing uniform, bright luminescence.

II. FABRICATION OF CNT COMPOSITE AND FIELD-EMISSION DEVICE STRUCTURE

Multiwalled CNTs with an average diameter of approximately 100 nm were mixed with EPDM rubber on a 6-in. two-roll mill. The weight ratio of CNT in this mixture was varied in the range of 0 – 53.8 wt. %. In the first kneading process at a mill opening of 2 mm, the molecular chains of EPDM are cut randomly and can easily creep into the CNT aggregates. When the mill opening is tightened to 0.1 mm, a strong force causes disentanglement of CNTs in the EPDM matrix. Detailed fabrication processes of the composite sheet were reported in Ref. 14. In the present study, the effect of the sheet thickness on the field emission properties has been investigated. The sheet thicknesses are 200 and 1000 μ m. The CNT/EPDM composite sheet was cut using a stainless razor. The density of the CNT tips is much higher on the cutting side than on the sheet surface because the roll-milling process forces the CNTs to orient along the direction of the CNT concentration; the resistivity substantially changes from an almost infinite value for EPDM to approximately 10 Ω cm for the composite with 53.8 wt. %.

^{a)}Electronic mail: kita@eedept.kobe-u.ac.jp.

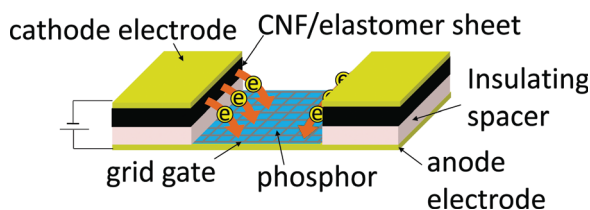


FIG. 1. (Color online) Field emission device using the side electron emission configuration.

III. RESULTS AND DISCUSSION

A. Effects of field concentration on electron emission

Figure 1 shows the field emission device structure used in our study. The device consists of a cathode, CNT/EPDM composite sheets as an electron emitter, a thin insulating spacer sheet, and a grid gate electrode placed on a phosphor-coated anode. The grid gate was placed in electrical contact with the anode. The CNT/EPDM composite sheet was cut into a size of $5 \times 1 \text{ mm}^2$. The composite sheet surface is sandwiched by the electrodes, and the cross-sectional cutting side efficiently emits electrons. Field-emission current was measured at room temperature by applying a negative bias to the emitter against the grid gate in a vacuum of $6.5 \times 10^{-4} \text{ Pa}$.

In conventional field-emission devices, where the cathode and anode are arranged facing each other, the electric field is uniform on the cathode surface. On the other hand, the electric field in the side-electron emission configuration (Fig. 1) is considered to be distributed as a function of its distance from the anode. Here, we theoretically calculated field distribution using a finite difference method. The calculation result is shown in Fig. 2. The horizontal ground level is the surface of the anode, and a composite sheet is placed at $Y = 500 \mu\text{m}$ above the anode, as indicated by the dashed line in the figure. The thickness of the sheet is assumed to be 1 mm. In this calculation, we assumed that the composite sheet is a low-resistance, good electrical conductor to simplify the analysis, and we took into account the dielectric constant, $\epsilon_r = 3.2$, of the spacer layer of polyether ether ketone (PEEK) resins in between the emitter and the electrode. The contrast of the counter image corresponds to the electric field; the bright color represents the high electric field region. The maximum field was $7.5 \text{ V}/\mu\text{m}$. The electric field is

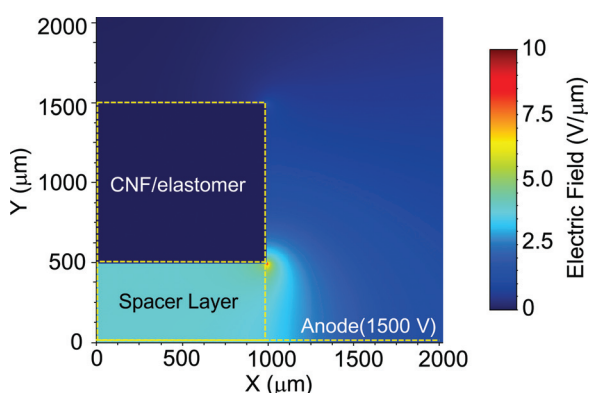


FIG. 2. (Color online) Calculated field distribution in the side-electron emission configuration.

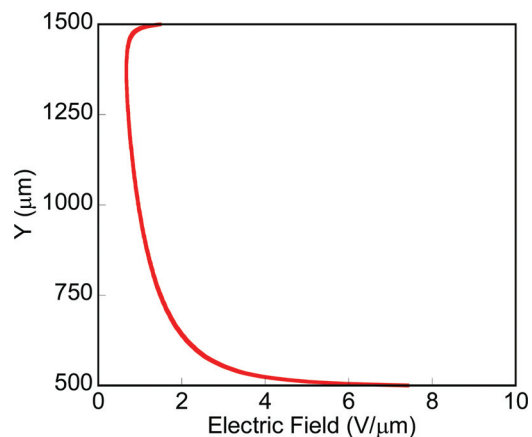


FIG. 3. (Color online) Electric field intensity at the cross-sectional cutting side of the composite sheet.

strongly concentrated at the bottom edge ($Y = 500 \mu\text{m}$) of the composite sheet. Figure 3 shows the change along the Y direction; the maximum electric field of $7.5 \text{ V}/\mu\text{m}$ at $Y = 500 \mu\text{m}$ rapidly decreases with the increase in the distance Y and becomes less than $1 \text{ V}/\mu\text{m}$ at $Y > 1000 \mu\text{m}$.

Field-emission characteristics have been investigated to verify the effect of the calculated field concentration. Figure 4 shows the experimental results of the field-emission characteristics of composite sheets with different thicknesses. In the figure, the blue and red symbols represent the results for the composite sheets with 200 and $1000 \mu\text{m}$ thicknesses, respectively. The threshold voltage of both devices with the different sheet thicknesses was approximately 200 V, which is sufficiently low as compared to that of conventional free-standing CNTs. A high emission current of over 1 mA was achieved when the applied voltage was over 1200 V. It is noted that the I - V curves for different sheet thicknesses are almost the same. This result suggests that field emission characteristics roughly correspond to the high field region near the bottom edge of the composite sheet.

Next, we discuss the effect of the insulating spacer layer thickness on the emission properties. Figure 5(a) shows the Fowler-Nordheim (FN) plots for different spacer thicknesses. The thickness of the composite sheet used here is $200 \mu\text{m}$.

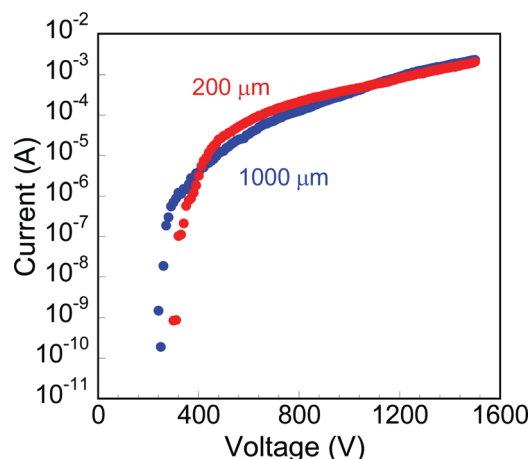


FIG. 4. (Color online) Field emission characteristics for different thicknesses of the composite sheet.

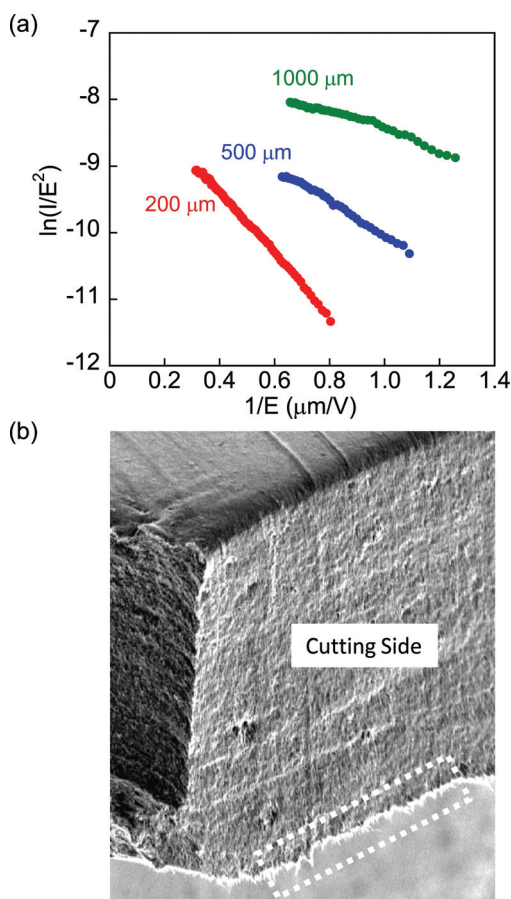


FIG. 5. (Color online) (a) FN analysis of emission characteristic as a function of the spacer thickness. (b) SEM image of cross-sectional cutting side of a EPDM sheet.

The change in the slope is very clear; it indicates that the local electric field at the CNT tips increases with the spacer layer thickness. According to Ref. 15, the field-concentration factor is nearly independent of the distance between the cathode and anode when this distance is three times longer than the CNT length. In our case, the distance (spacer-layer thickness) is sufficiently longer than the CNT length of approximately 10–20 μm . Thus, the presented results indicate that the simple field-concentration model assuming bare CNTs standing on a flat substrate cannot be applied to interpret the results. On the other hand, CNTs protruding from the cutting side of the composite sheet show relatively large edge structures, as shown in Fig. 5(b). Such morphological structures can be attributed to the change in the field-concentration factor as a function of the spacer-layer thickness in the range of 200–1000 μm .

B. Trajectory of emitted electrons and design of the cathode in field emission device

Next, we discuss the trajectories of emitted electrons in order to realize uniform and efficient light emission. Figure 6(a) shows the typical light emission pattern of our device. The composite sheets (indicated by white dotted squares) are placed beneath the cathode at a distance of 8 mm. Bright areas correspond to regions where the excitation electron density is high. All regions within a distance of approxi-

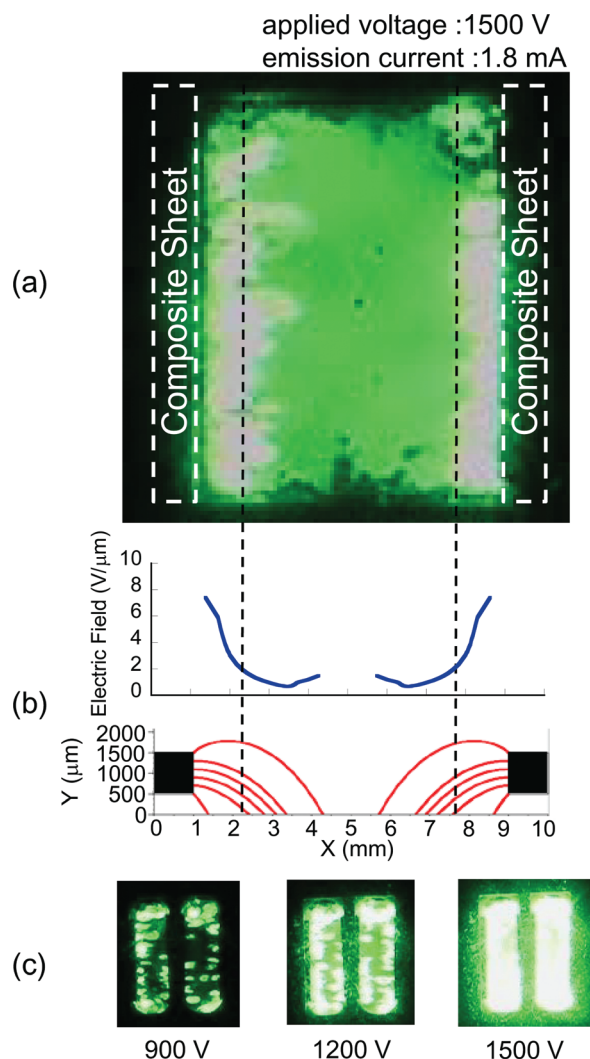


FIG. 6. (Color online) (a) Light emission image from the side-electron emission configurational device. (b) The trajectories of electrons emitted from the cross-sectional cutting side and a profile of the electric field at the cross-sectional cutting side as a function of X . (c) Light emission images at respective applied voltages from the optimized side-electron emission configurational device.

mately 1.5 mm from the electrode are very bright. Therefore, strong electron excitation occurs at the area close to the composite sheet. To confirm that the region is efficiently excited, we calculated the trajectory of the emitted electrons. The results are shown in Fig. 6(b). Black squares indicate the composite sheet placed on both sides. Red lines represent the calculated trajectories of the emitted electrons. The trajectory lines are drawn after every 200 μm . Blue lines indicate the electric field strength, E , as a function of X . According to the FN relation, the current density is proportional to $E^2 \exp(-1/E)$. The lateral distance of the trajectory depends on its position at the cross-sectional cutting side of the composite sheet; electrons emitted from the bottom of the composite sheet are accelerated strongly and excite the area close to the sheet. On the other hand, electrons emitted from the top reach the area far from the edge of the composite sheet, but the accelerating electric field is weak; thus, only the area near the composite sheet becomes bright. The bright area becomes wider with increase in the applied voltage. Since

the region within the distance of approximately 1.5 mm from the electrode is very bright, we designed a new electrode, shown in Fig. 6(c), the lateral distance of which is reduced to 3.5 mm. The bright area becomes wider with the increase in the applied voltage, and finally, at 1500 V, a uniform bright emission has been achieved. At this condition, the luminance from green phosphor of ZnS:Cu,Al (P22-G4) exceeded 37000 cd/m².

IV. SUMMARY

We investigated field-emission properties of a CNT/EPDM composite in a side-electron emission configuration. Theoretical calculations of the electric field distributed on the emission surface indicated that the electric field is concentrated near the edge close to the anode. We found that the local electric field increases with the spacer-layer thickness; this property is beneficial in fabricating large-scale devices with a uniform emission pattern. We optimized the device structure with a side-electron emission configuration and obtained a uniform light emission using a bridge-type cathode. We have demonstrated bright emission over 37000 cd/m² with the optimized device structure.

- ¹J. Xiong, Z. Zheng, X. Qin, M. Li, and X. Wang, *Carbon* **44**, 2701 (2006).
- ²A. Allaoui, S. Bai, H. M. Cheng, and J. B. Bai, *Compos. Sci. Technol.* **62**, 1993 (2002).
- ³W. Chen, X. Tao, P. Xue, and X. Cheng, *Appl. Surf. Sci.* **252**, 1404 (2005).
- ⁴J. K. W. Sandler, J. E. Kirk, I. A. Kinloch, M. S. P. Shaffer, and A. H. Windle, *Polymer* **44**, 5893 (2003).
- ⁵C. H. Liu, H. Huang, Y. Wu, and S. S. Fan, *Appl. Phys. Lett.* **84**, 4248 (2004).
- ⁶T. Kita, Y. Hayashi, O. Wada, H. Yanagi, Y. Kawai, A. Magario, and T. Noguchi, *Jpn. J. Appl. Phys.* **45**, L1186 (2006).
- ⁷M. Kawamura, Y. Tanaka, T. Kita, O. Wada, H. Nakamura, H. Yanagi, A. Magario, and T. Noguchi, *Appl. Phys. Express* **1**, 074004 (2008).
- ⁸T. Sekitani, Y. Noguchi, K. Hata, T. Fukushima, T. Aida, and T. Someya, *Science* **321**, 1468 (2008).
- ⁹Y. Saito, S. Uemura, and K. Hamaguchi, *Jpn. J. Appl. Phys.* **37**, L346 (1998).
- ¹⁰M. Croci, I. Arfaoui, T. Stöckli, A. Chatelain, and J.-M. Bonard, *Microelectron. J.* **35**, 329 (2004).
- ¹¹S. Fan, M. G. Chapline, N. R. Franklin, T. W. Tombler, A. M. Cassell, and H. Dai, *Science* **283**, 512 (1999).
- ¹²W. Zhu, C. Bower, O. Zhou, G. Kochanski, and S. Jin, *Appl. Phys. Lett.* **75**, 873 (1999).
- ¹³H. Nakamura, H. Yanagi, T. Kita, A. Magario, and T. Noguchi, *Appl. Phys. Lett.* **92**, 243302 (2008).
- ¹⁴T. Noguchi, A. Magario, S. Fukuzawa, S. Shimizu, J. Beppu, and M. Seki, *Mater. Trans.* **45**, L1186 (2004).
- ¹⁵R. C. Smith, D. C. Cox, and S. R. P. Silva, *Appl. Phys. Lett.* **87**, 103112 (2005).